Kaon condensation and composition of neutron star matter in a modified quark-meson coupling model

C. Y. Ryu,[1,*,†] C. H. Hyun,[1,2,‡] S. W. Hong,[3,§] and B. T. Kim[1,‖]
[1]*Department of Physics and Institute of Basic Science, Sungkyunkwan University, Suwon 440-746, Korea*
[2]*School of Physics, Seoul National University, Seoul 151-742, Korea*
[3]*Department of Physics and Basic Atomic Energy Research Institute, Sungkyunkwan University, Suwon 440-746, Korea*
(Received 11 August 2006; revised manuscript received 29 January 2007; published 7 May 2007)

We use the modified quark-meson coupling (MQMC) model to study the composition profile of neutron star matter and compare the results with those calculated by quantum hadrodynamics (QHD). Both MQMC and QHD model parameters are adjusted to produce exactly the same saturation properties so that we can investigate the model dependences of the matter composition at high densities. We consider the possibility of deep kaon optical potential and find that the composition of matter is very sensitive to the interaction strength of kaons with matter. The onset densities of the kaon condensation are studied in detail by varying the kaon optical potentials. We find that the MQMC model produces the kaon condensation at lower densities than QHD. The presence of kaon condensation changes drastically the population of octet baryons and leptons. Once the kaon condensation takes place, the population of kaons builds up very quickly, and kaons become the dominant component of the matter. We find that the ω meson plays an important role in increasing the kaon population and suppressing the hyperon population.

DOI: 10.1103/PhysRevC.75.055804 PACS number(s): 26.60.+c, 21.65.+f, 12.39.Ki, 13.75.Jz

I. INTRODUCTION

Observation of neutron star properties such as mass, size, and temperature provides us with important clues to the understanding of the state of matter at extremely high densities. In the 1970s, the maximum mass of the neutron star was calculated with the NN potentials available at that time [1–4] and mean field models [5,6]. Most of the calculations done in the 1970s resulted in stiff equations of state, and thus the maximum mass of a neutron star was predicted to be larger than $2M_\odot$, where $M_\odot$ is the solar mass. Only the Reid soft core potential yielded a soft equation of state and consequently a small maximum mass of a neutron star, $1.6M_\odot$ [1]. Recent observations of the masses of binary pulsars [7], which are candidates of neutron stars, indicate that the maximum mass of neutron stars are roughly around $1.5M_\odot$, substantially smaller than most of the values predicted in the 1970s. (However, very recent observations seem to suggest the possible existence of more massive pulsars in the range $(1.8–2.0)M_\odot$ [8,9], though further confirmation is needed.) On the other hand, exotic forms of matter, i.e., matter consisting of degrees of freedom other than the nucleons, were proposed many years ago. Some of the proposed exotic states of matter include those with the creation of hyperons [10], Bose-Einstein condensation (pions [11] or kaons [12]), strange matter [13], and quark deconfinement [14–16]. These exotic states seem to reduce the maximum mass of a neutron star close to the observations [17–19], implying that exotic degrees of freedom seem to be needed to reproduce the observed masses of neutron stars.

In this work, we consider the strangeness degrees of freedom by including both hyperon creation and kaon condensation in the neutron star matter. (It is the antikaon that matters here, but we simply refer to both kaons and antikaons as kaons for brevity.) The masses and energies of the hyperons and kaons in the medium are sensitive to their interactions with the surrounding matter. In the meson-exchange picture, meson-hyperon and meson-kaon coupling constants can fix the strength of these interactions. The meson-hyperon coupling constants may be determined from the binding energies of hyperons in hypernuclei. The meson-kaon coupling constants have been studied by using the kaon-nucleon scattering [20,21] and kaonic atom data [20]. Recently, the magnitudes of the kaon-nucleus potential in matter have attracted much attention. Some calculations [20,22,23] show that the real part of the K^--nucleus optical potential U_{K^-} is shallow ($U_{K^-} \approx -50$ MeV), but some other calculations suggest that U_{K^-} can be as large as about -120 MeV [21,24] or even close to -200 MeV [25].

Akaishi and Yamazaki predicted possible existence of deeply bound kaonic nuclei [26], in which U_{K^-} at normal density ρ_0 was estimated to be about -120 MeV. Then, experiments at KEK claimed the observation of tribaryon kaonic nuclei, S^0 [27] and S^+ [28], which seemed to suggest that K^- may be even more deeply bound than the theoretical prediction [26] (The former claim [27], however, was withdrawn by the experimental group [29]). FINUDA Collaboration at DAΦNE [30] and a BNL experiment with $^{16}O(K^-, n)$ reaction [31] also reported distinct peaks. More recently, there was a theoretical work which considered large kaonic binding energies and calculated widths of kaonic nuclear bound states [32]. The identities of these experimental peaks need to be studied further experimentally and theoretically. However, in this work, we consider the possibility of deep optical potential

*Present address: Research Center for Nuclear Physics, Osaka University, Ibaraki, Osaka 567-0047, Japan
†Electronic address: cyryu@rcnp.osaka-u.ac.jp
‡Electronic address: hch@meson.skku.ac.kr
§Electronic address: swhong@skku.ac.kr
‖Electronic address: btkim@skku.ac.kr

of kaons in nuclei and explore the consequences in the composition profile of neutron star matter.

In this work, for the description of dense matter we employ the modified quark-meson coupling (MQMC) model [33]. Nucleons and hyperons in the baryon octet are treated as MIT bags. The bag constant B_B and phenomenological constant Z_B for a baryon B are fixed to reproduce the free mass of each baryon B. Coupling constants between (u, d) quarks in the bags and (σ, ω, ρ) mesons are adjusted to give us the binding energy per a nucleon $E_b/A = 16$ MeV and symmetry energy $a_{\rm sym} = 32.5$ MeV at the saturation density $\rho_0 = 0.17$ fm^{-3}. Since the interaction between the s quark and mesons are not well known, we adopt the standard quark counting rule and assume the s quark is decoupled from (σ, ω, ρ) mesons. To take into account the interactions between s quarks, we introduce $\sigma^*(980)$ and $\phi(1020)$ mesons following Ref. [18] for the baryon and Ref. [34] for the kaon. We also assume the kaon as a point particle. This treatment allows us to use U_{K^-} as an input to fix the coupling constant between the σ meson and the kaon, $g_{\sigma K}$. In our model, the real part of the kaon optical potential at $\rho = \rho_0$ can be written as $U_{K^-} = -[g_{\sigma K}\sigma(\rho_0) + g_{\omega K}\omega(\rho_0)]$, where $\sigma(\rho_0)$ and $\omega(\rho_0)$ are the values of the meson fields at ρ_0. Using the value of $g_{\omega K}$ given by the quark counting rule, we can fix $g_{\sigma K}$ for each given value of U_{K^-}. Once the parameters of the model are fixed, the composition profile of neutron star matter can be obtained from the β equilibrium and charge neutrality. We find that the composition of neutron star matter changes dramatically depending on the value of U_{K^-}.

To investigate the model dependence of the results, we also employ the quantum hadrodynamics (QHD) model [35] for calculating the composition of matter. The parameters of the QHD model are calibrated to produce exactly the same saturation properties as in the MQMC model. Our calculations show that the onset densities of the kaon condensation and the compositions of matter at high densities are substantially model dependent. In Sec. II, we introduce model Lagrangians and fix the model parameters. The results are discussed in Sec. III. Conclusions and discussions follow in Sec. IV.

II. THEORY

In this section, we first briefly sketch the MQMC and QHD models by presenting the model Lagrangians. The models are calibrated so as to be consistent with each other at the saturation density by fixing the coupling constants of both models to produce exactly the same saturation properties: the saturation density, binding energy, symmetry energy, nucleon effective mass, and compression modulus. We then show how the physical quantities that will determine the composition of the neutron star matter can be obtained self-consistently.

A. Models

The model Lagrangian comprises the terms for the octet baryons, exchange mesons, leptons, and kaons, $\mathcal{L}_{\rm tot} = \mathcal{L}_B + \mathcal{L}_M + \mathcal{L}_l + \mathcal{L}_K$. Octet baryon, exchange meson, and lepton terms in the mean field approximation can be written as

$$\mathcal{L}_B = \sum_B \bar{\psi}_B \Big[i\gamma\cdot\partial - m_B^*(\sigma,\sigma^*) - \gamma^0\Big(g_{\omega B}\omega_0 + g_{\phi B}\phi_0 + \frac{1}{2}g_{\rho B}\tau_z\rho_{03}\Big)\Big]\psi_B, \quad (1)$$

$$\mathcal{L}_M = -\frac{1}{2}m_\sigma^2\sigma^2 - \frac{1}{2}m_{\sigma^*}^2\sigma^{*2} + \frac{1}{2}m_\omega^2\omega_0^2 + \frac{1}{2}m_\phi^2\phi_0^2 + \frac{1}{2}m_\rho^2\rho_{03}^2, \quad (2)$$

$$\mathcal{L}_l = \sum_l \bar{\psi}_l(i\gamma\cdot\partial - m_l)\psi_l, \quad (3)$$

where B denotes the sum over all the octet baryons $(p, n, \Lambda, \Sigma^+, \Sigma^0, \Sigma^-, \Xi^0, \Xi^-)$, and l stands for the sum over the free electrons and muons (e^-, μ^-). σ, ω, and ρ mesons mediate the interactions between the nonstrange light quarks (u and d). σ^* and ϕ mesons are introduced to take into account the interactions between s quarks. $\mathcal{L}_B$ is of the identical form for both the MQMC and QHD models, but differs in the definition of the effective baryon mass m_B^* as will be shown below.

1. MQMC

In the MQMC model, a baryon is a composite system with quarks in a spherical bag, and its mass is given in terms of bag parameters and quark eigenenergy. The effective mass of a baryon in matter $m_B^*(\sigma, \sigma^*)$ can be written as [18,33,36–38]

$$m_B^* = \sqrt{E_B^2 - \sum_q \Big(\frac{x_q}{R}\Big)^2}. \quad (4)$$

The bag energy of a baryon is given by

$$E_B = \sum_q \frac{\Omega_q}{R} - \frac{Z_B}{R} + \frac{4}{3}\pi R^3 B_B, \quad (5)$$

where B_B and Z_B are the bag constant and a phenomenological constant for the zero-point motion of a baryon B, respectively. $\Omega_q = \sqrt{x_q^2 + (Rm_q^*)^2}$, where $m_q^*(= m_q - g_\sigma^q\sigma - g_{\sigma^*}^q\sigma^*)$ is the effective mass of a quark whose free mass is m_q. We take $m_q = 0$ for $q = u, d$ and $m_q = 150$ MeV for $q = s$. (Other choices of $m_{q=s}$ values do not make differences in the results [39].) x_q is determined from the boundary condition on the bag surface $r = R$,

$$j_0(x_q) = \beta_q j_1(x_q), \quad (6)$$

where $\beta_q = \sqrt{\frac{\Omega_q - Rm_q^*}{\Omega_q + Rm_q^*}}$. In the MQMC model, the bag constant B_B is assumed to depend on density [33,38]. In this work, we use the extended form in Ref. [18] to include the contribution from σ^* as

$$B_B(\sigma,\sigma^*) = B_{B0}\exp\left\{-\frac{4}{m_B}\left[g_\sigma'^B\sum_{q=u,d} n_q\sigma + g_{\sigma^*}'^B\left(3 - \sum_{q=u,d} n_q\right)\sigma^*\right]\right\}, \quad (7)$$

where m_B is the free mass of the baryon B, assuming that the σ meson couples to u and d quarks only and that the σ^* meson couples to the s quark only.

2. QHD

In the QHD model, a baryon is treated as a point particle, and thus its effective mass is simply written as

$$m_B^* = m_B - g_{\sigma B}\sigma - g_{\sigma^* B}\sigma^*. \tag{8}$$

To reproduce the same saturation properties as obtained in the MQMC model, self-interactions of the σ field [40]

$$U_\sigma^{\rm QHD} = \tfrac{1}{3}g_2\sigma^3 + \tfrac{1}{4}g_3\sigma^4 \tag{9}$$

are added to Eq. (2) so that

$$\mathcal{L}_M^{\rm QHD} = \mathcal{L}_M - U_\sigma^{\rm QHD}. \tag{10}$$

As mentioned above, the baryon and the lepton Lagrangians for the QHD model take the form given by Eqs. (1) and (3).

3. Kaon

The effective Lagrangian for the kaon may be expressed as [41]

$$\mathcal{L}_K = D_\mu^* K^* D^\mu K - {m_K^*}^2 K^* K, \tag{11}$$

where $D_\mu = \partial_\mu + i g_{\omega K}\omega_\mu - i g_{\phi K}\phi_\mu + i\frac{1}{2}g_{\rho K}\vec{\tau}\cdot\vec{\rho}_\mu$. In this work, we treat the kaon as a point particle in both MQMC and QHD models, and its effective mass is given by

$$m_K^* = m_K - g_{\sigma K}\sigma - g_{\sigma^* K}\sigma^*. \tag{12}$$

The equation of motion for a kaon is given by

$$[D_\mu D^\mu + {m_K^*}^2]K(x) = 0. \tag{13}$$

In uniform infinite matter, the kaon field $K(x)$ can be written as a plane wave. Substituting the plane wave solution into the equation of motion, we obtain the dispersion relation for the antikaon

$$\omega_K = m_K^* - g_{\omega K}\omega_0 + g_{\phi K}\phi_0 - g_{\rho K}\tfrac{1}{2}\rho_{03}. \tag{14}$$

B. Model parameters

1. MQMC

In the MQMC model, MIT bag parameters B_{B0} and Z_B are determined to reproduce the free mass of a baryon B, $m_B^*|_{\rho=0} = m_B$ with the minimization condition $\frac{\partial m_B}{\partial R}|_{R=R_0} = 0$ at a free bag radius R_0, which we choose as $R_0 = 0.6$ fm. The bag parameters B_{B0} and Z_B for the octet baryons are listed in Table I.

Three saturation conditions ρ_0, E_b/A, and $a_{\rm sym}$ could determine three quark-meson coupling constants $g_\sigma^{u,d}$, $g_\omega^{u,d}$, and $g_\rho^{u,d}$, assuming u and d quarks to be identical in the isodoublet. The MQMC model, however, introduces an additional constant ${g'}_\sigma^B$ in Eq. (7). Thus we fix $g_\sigma^{u,d} = 1$, and adjust the remaining three constants to meet the three conditions. The resulting coupling constants are given in Table II together with the ratio of the effective mass of the nucleon m_N^*/m_N and the compression modulus K. m_N^* and K are within reasonable ranges: $m_N^* = (0.7 \sim 0.8)m_N$ and $K = 200 \sim 300$ MeV.

TABLE I. Bag constants B_{B0} and phenomenological constants Z_B for octet baryons to reproduce the free mass of each baryon. Bag radius is chosen as $R_0 = 0.6$ fm for all octet baryons; bare masses of quarks are fixed as $m_{u(d)} = 0$ MeV and $m_s = 150$ MeV.

B	m_B (MeV)	$B_{B0}^{1/4}$ (MeV)	Z_B
N	939.0	188.1	2.030
Λ	1115.6	197.6	1.926
Σ^0	1192.0	202.9	1.826
Σ^-	1197.3	203.3	1.819
Ξ^0	1314.7	207.6	1.775
Ξ^-	1321.3	208.0	1.765

The coupling constants between s quarks and mesons cannot be determined from the saturation properties. In principle, experimental data from hypernuclei and kaon-nucleus scattering could be used to determine the coupling constants between s quarks and mesons (for example, see Ref. [42]). However, these coupling constants are not well known yet, and for simplicity we assume that the quark counting rule holds and that the s quark does not interact with u and d quarks. Then we have

$$g_\sigma^s = g_\omega^s = g_\rho^s = g_{\sigma*}^{u,d} = g_\phi^{u,d} = 0. \tag{15}$$

To fix the meson-baryon coupling constants in the model Lagrangian, we also use the quark counting rule

$$\begin{aligned} \tfrac{1}{3}g_{\omega N} &= \tfrac{1}{2}g_{\omega\Lambda} = \tfrac{1}{2}g_{\omega\Sigma} = g_{\omega\Xi} = g_\omega^q, \\ g_{\rho N} &= g_{\rho\Sigma} = g_{\rho\Xi} = g_\rho^q, \quad g_{\rho\Lambda} = 0, \\ g_{\phi\Lambda} &= g_{\phi\Sigma} = \tfrac{1}{2}g_{\phi\Xi} = g_\phi^s, \end{aligned} \tag{16}$$

and the SU(6) symmetry

$$\begin{aligned} g_{\sigma*}^s &= \sqrt{2}g_\sigma^{u,d} = \sqrt{2}, \\ g_\phi^s &= \sqrt{2}g_\omega^{u,d} = 3.83, \\ {g'}_{\sigma^*}^B &= \sqrt{2}{g'}_\sigma^B. \end{aligned} \tag{17}$$

The quark-meson coupling constants g_ω^q and g_ρ^q given in Table II and the relations in Eqs. (15)–(17) determine all the meson-baryon coupling of the MQMC model.

TABLE II. Coupling constants between (u, d) quarks and (σ, ω, ρ) mesons in the MQMC model to reproduce the binding energy $E_b/A = 16$ MeV and symmetry energy $a_{\rm sym} = 32.5$ MeV at the saturation density 0.17 fm^{-3}. m_N^*/m_N and K are the ratio of the effective mass to the free mass of the nucleon and the compression modulus at the saturation density, respectively.

g_σ^q	g_ω^q	${g'}_\sigma^B$	g_ρ^q	m_N^*/m_N	K (MeV)
1.0	2.71	2.27	7.88	0.78	285.5

TABLE III. Meson-nucleon coupling constants and coefficients of the σ-meson self-interaction terms used in the QHD model. They reproduce the same saturation properties as in the MQMC model: $\rho_0 = 0.17$ fm^{-3}, $E_b = 16A$ MeV, $a_{\rm sym} = 32.5$ MeV, $m_N^* = 0.78 m_N$, and $K = 285.5$ MeV.

$g_{\sigma N}$	$g_{\omega N}$	$g_{\rho N}$	g_2 (fm^{-1})	g_3
8.06	8.19	7.88	12.139	48.414

2. QHD

In the QHD model, $g_{\sigma N}$ and $g_{\omega N}$ are adjusted to yield ρ_0 and E_b, and $g_{\rho N}$ is fitted to produce $a_{\rm sym}$. g_2 and g_3 in $U_\sigma^{\rm QHD}$ of Eq. (9) are fixed to reproduce the same m_N^* and K values as listed in Table II for the MQMC model. The coupling constants determined in this way are given in Table III. In the MQMC model, meson-baryon coupling constants are obtained from the quark-meson coupling constants. On the other hand, in QHD meson-nucleon coupling constants provide the starting point for the determination of the other remaining meson-baryon coupling constants. Once meson-nucleon coupling constants are fixed from the saturation properties, meson-hyperon coupling constants can be obtained by the quark counting rule (as in Eq. (16)) and the SU(6) symmetry (as in Eq. (17)). The coupling constants between strange mesons and hyperons can be obtained by combining the quark counting rule and the SU(6) symmetry, e.g., $g_{\phi\Lambda} = \sqrt{2} g_{\omega N}/3$ and $g_{\sigma^*\Lambda} = \sqrt{2} g_{\sigma N}/3$.

3. Kaon

There are five kaon-meson coupling constants in our models: $g_{\sigma K}$, $g_{\omega K}$, $g_{\rho K}$, $g_{\sigma^* K}$, and $g_{\phi K}$. The constants $g_{\omega K}$ and $g_{\rho K}$ can be fixed from the quark counting rule: $g_{\omega K} = g_\omega^q$ and $g_{\rho K} = g_\rho^q$ for the MQMC model, and $g_{\omega K} = g_{\omega N}/3$ and $g_{\rho K} = g_{\rho N}$ for QHD. (Obviously $g_{\rho K}$ from the MQMC model is the same as that from QHD, and $g_{\omega K} (= 2.71)$ from the MQMC model is essentially the same as $g_{\omega K} (= 2.73)$ from QHD.) $g_{\sigma^* K}$ may be fixed from $f_0(980)$ decay [43], and $g_{\phi K}$ from the SU(6) relation $\sqrt{2} g_{\phi K} = g_{\pi\pi\rho} = 6.04$ [44]. $g_{\sigma^* K}$ and $g_{\phi K}$ thus fixed are 2.65 and 4.27, respectively. The remaining coupling constant, $g_{\sigma K}$, can be related to the real part of the optical potential of a kaon at the saturation density through $U_{K^-} = -(g_{\sigma K}\sigma + g_{\omega K}\omega_0)$. $g_{\sigma K}$ values corresponding to several values of U_{K^-} are listed in Table IV for both MQMC and QHD models.

Thus, out of five kaon-meson coupling constants, $g_{\rho K}$, $g_{\sigma^* K}$, and $g_{\phi K}$ are the same for both models. $g_{\omega K}$ values are essentially the same for both models. Also, $g_{\sigma K}$ values are very similar in both models for all U_{K^-} values as seen in Table IV. Therefore, all five kaon-meson coupling constants are practically the same for both MQMC and QHD models.

TABLE IV. $g_{\sigma K}$ determined for several U_{K^-} values in the MQMC and QHD models.

U_{K^-} (MeV)	-80	-100	-120	-140	-160
$g_{\sigma K}$ (MQMC)	1.25	2.01	2.75	3.50	4.25
$g_{\sigma K}$ (QHD)	1.26	2.04	2.82	3.61	4.39

C. Other quantities relevant to neutron star matter

To obtain the composition of neutron star matter, we need to determine 16 unknown variables at each matter density, which include five meson fields ($\sigma, \omega, \rho, \sigma^*, \phi$), eight octet baryon densities, two lepton densities, and the kaon density ρ_K. Five meson fields can be determined from their equations of motion:

$$m_\sigma^2 \sigma + \frac{\partial}{\partial\sigma} U_\sigma^{\rm QHD} = \sum_B g_{\sigma B} C_B(\sigma) \frac{2J_B+1}{2\pi^2} \times \int_0^{k_B} \frac{m_B^*}{\left[k^2 + m_B^{*2}\right]^{1/2}} k^2 dk + g_{\sigma K}\rho_K, \tag{18}$$

$$m_{\sigma^*}^2 \sigma^* = \sum_B g_{\sigma^* B} C_B(\sigma^*) \frac{2J_B+1}{2\pi^2} \times \int_0^{k_B} \frac{m_B^*}{\left[k^2 + m_B^{*2}\right]^{1/2}} k^2 dk + g_{\sigma^* K}\rho_K, \tag{19}$$

$$m_\omega^2 \omega_0 = \sum_B g_{\omega B}(2J_B+1)k_B^3/(6\pi^2) - g_{\omega K}\rho_K, \tag{20}$$

$$m_\phi^2 \phi_0 = \sum_B g_{\phi B}(2J_B+1)k_B^3/(6\pi^2) + g_{\phi K}\rho_K, \tag{21}$$

$$m_\rho^2 \rho_{03} = \sum_B g_{\rho B} I_{3B}(2J_B+1)k_B^3/(6\pi^2) - g_{\rho K} \times \frac{1}{2}\rho_K, \tag{22}$$

where J_B and I_{3B} are the spin and the isospin projection, respectively, and k_B is the Fermi momentum of the baryon B. In Eq.(18), $\frac{\partial}{\partial\sigma} U_\sigma^{\rm QHD}$ term needs to be there only for QHD and is not to be included in the MQMC model. $C_B(\sigma)$ and $C_B(\sigma^*)$ are determined from the relations $g_{\sigma B} C_B(\sigma) = -\frac{\partial m_B^*}{\partial\sigma}$ and $g_{\sigma^* B} C_B(\sigma^*) = -\frac{\partial m_B^*}{\partial\sigma^*}$. For QHD, $C_B(\sigma) = C_B(\sigma^*) = 1$. For MQMC, the explicit forms of $C_B(\sigma)$ and $C_B(\sigma^*)$ are given in Ref. [18].

Charge neutrality condition of neutron star matter is expressed as

$$\sum_B q_B \rho_B - \rho_K - \rho_e - \rho_\mu = 0, \tag{23}$$

where q_B is the charge of baryon B and ρ_B is the number density of B. Using the charge neutrality and the baryon number conservation conditions, one can fix two quantities, e.g., the density of the neutron and the electron. With these two variables fixed, β equilibrium conditions of the baryons give us the following seven relations for the chemical potentials

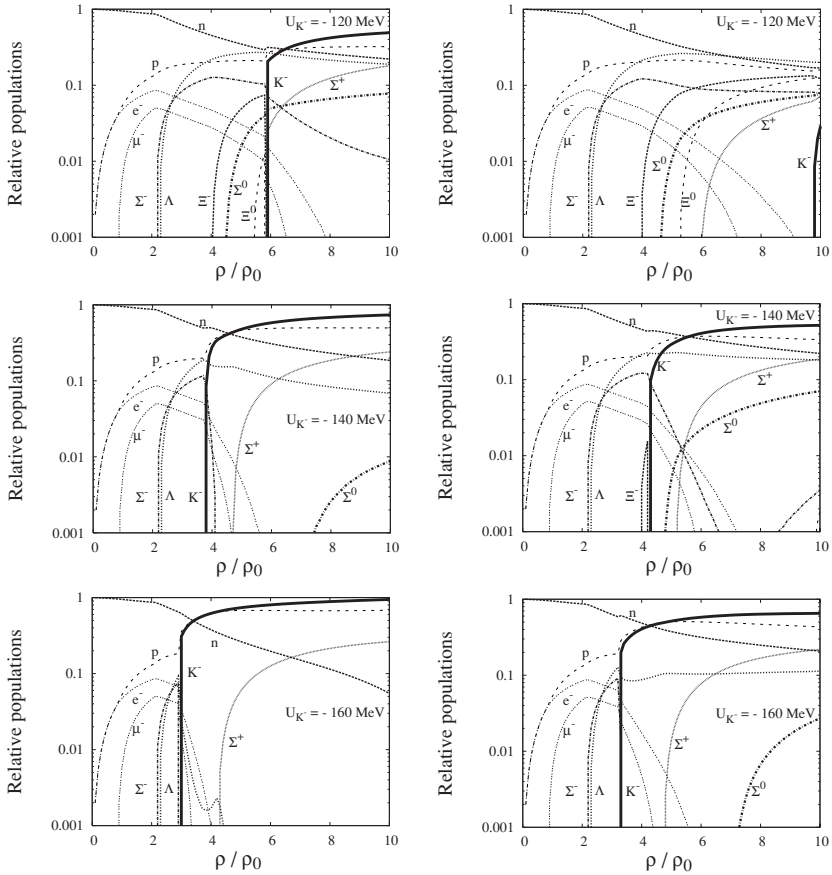

FIG. 1. Compositions of neutron star matter calculated from MQMC (left panels) and QHD (right panels) models.

of p, Λ, Σ^+, Σ^-, Σ^0, Ξ^-, and Ξ^0 as

$$\begin{aligned} \mu_n &= \mu_\Lambda = \mu_{\Sigma^0} = \mu_{\Xi^0}, \\ \mu_n + \mu_e &= \mu_{\Sigma^-} = \mu_{\Xi^-}, \\ \mu_n - \mu_e &= \mu_p = \mu_{\Sigma^+}, \end{aligned} \tag{24}$$

where the chemical potential of baryon B is given by $\mu_B = \sqrt{k_B^2 + m_B^{*2}(\sigma, \sigma^*)} + g_{\omega B}\omega_0 + g_{\phi B}\phi_0 + g_{\rho B} I_{3B}\rho_{03}$. The chemical potential of a noninteracting lepton l is simply written as $\mu_l = \sqrt{k_l^2 + m_l^2}$. The β-equilibrium condition for leptons

$$\mu_e = \mu_\mu \tag{25}$$

determines the density of muons. At a density where the condition

$$\omega_K = \mu_n - \mu_p \tag{26}$$

is satisfied, kaons are condensed, and the kaon density ρ_K becomes nonzero. Solving the Eqs. (18)–(26) self-consistently and simultaneously, one can determine the 16 variables uniquely.

III. RESULTS

Figure 1 shows the relative populations, the ratios of the densities of octet baryons, leptons, and K^- to the total baryon density, in the neutron star matter as functions of ρ/ρ_0 up to $\rho = 10\rho_0$. The left panels show the results from the MQMC model and the right from the QHD model for $U_{K^-} = -120$, -140, and -160 MeV. (Figures for $U_{K^-} = -80$ and -100 MeV are not shown here because they are not too much different from the one for $U_{K^-} = -120$ MeV particularly for QHD.) Figures from both models show that the onset density of the kaon condensation $\rho_{\rm crit}$ becomes lower as $|U_{K^-}|$ increases.

To see how $\rho_{\rm crit}$ changes depending on U_{K^-}, let us consider Eq. (26), which determines $\rho_{\rm crit}$. Figure 2 displays ω_K and

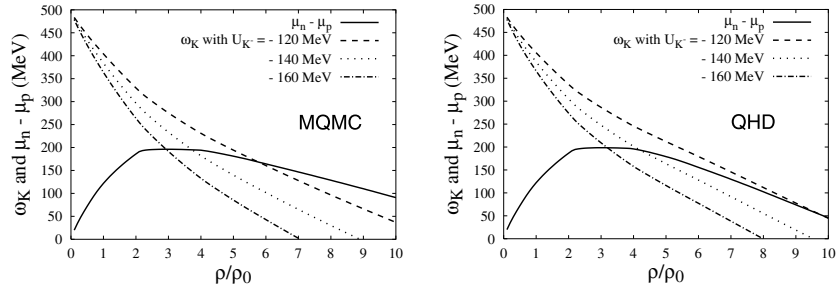

FIG. 2. Kaon energies ω_K for three U_{K^-} values. At densities where ω_K and $\mu_n - \mu_p$ intersect, kaons start to condense.

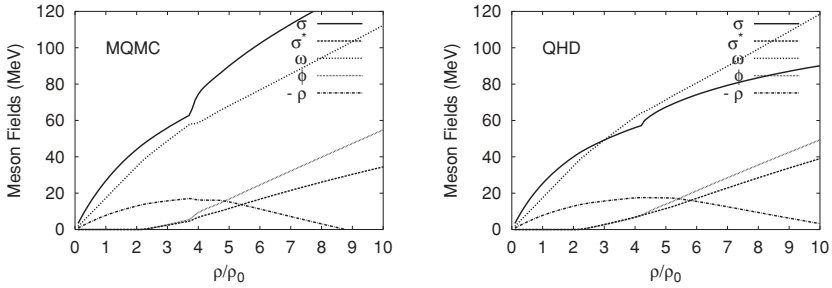

FIG. 3. Meson fields calculated from the MQMC and the QHD models as functions of the matter density for $U_{K^-} = -140$ MeV.

$\mu_n - \mu_p$, which are, respectively, the left and the right hand sides of Eq. (26) (computed without including kaon condensation just for producing this figure). The left panel is from the MQMC model, and the right panel from QHD. At a density where the curve of ω_K intersects with that of $\mu_n - \mu_p$, kaon condensation sets in. Among the coupling constants and meson fields that determine ω_K, only $g_{\sigma K}$ depends on U_{K^-}. The σ meson contributes to ω_K attractively, as can be seen in Eq. (14). Thus ω_K becomes smaller for a larger $|U_{K^-}|$, as shown in Fig. 2.

Figure 1 also shows that as $|U_{K^-}|$ increases from 120 to 140 MeV, $\rho_{\rm crit}$ changes drastically in both MQMC and QHD models; but as $|U_{K^-}|$ increases further above 140 MeV, $\rho_{\rm crit}$ changes only moderately. This can also be seen in Fig. 2. As $|U_{K^-}|$ increases from 120 to 140 MeV, the intersection between the curves for $\mu_n - \mu_p$ and ω_K moves rapidly (particularly for QHD); whereas when $|U_{K^-}|$ increases further above 140 MeV, the intersection shifts only a little to lower densities.

Another common feature of the two models is that regardless of $\rho_{\rm crit}$, once the kaon is created, the density of K^- piles up very quickly and overwhelms the population of the hyperons and even the nucleons. This behavior was also obtained by other authors [17,34,41,45]. The reason can be partly attributed to the ω meson. The ω-meson term in the energy of K^- [in Eq. (14)] has a negative sign and is thus attractive, but it is repulsive for octet baryons. Figure 3 shows the ω meson is a dominant meson at higher densities in both MQMC and QHD models. Thus the ω meson enhances the population of K^- but suppresses baryons, and the kaon density increases rapidly. In addition, due to the competition between the negatively charged hyperons and K^- in the charge neutrality condition, the negative hyperons are highly suppressed and in some cases not even created at all as soon as the kaon condensation sets in. Positively charged hyperons, on the other hand, receive the opposite effects from the kaon condensation, and Σ^+ is created at lower densities as $|U_{K^-}|$ increases more. The proton density is also enhanced by large abundance of K^-, which facilitates in turn the enhancement of Σ^+ population through the chemical equilibrium condition of the positively charged hyperons in Eq. (24).

Let us now discuss different aspects of the two model calculations. First, Fig. 1 shows that $\rho_{\rm crit}$ from the MQMC model is lower than that from QHD. For $U_{K^-} = -120$, -140, and -160 MeV, $\rho_{\rm crit}$ values are $5.9\rho_0$, $3.8\rho_0$ and $3.0\rho_0$ in the MQMC model, respectively, while they are $9.8\rho_0$, $4.3\rho_0$, and $3.3\rho_0$ in QHD. Secondly, the MQMC model predicts a larger population of the kaon than QHD for a given U_{K^-} value. Figure 2 shows that ω_K calculated from the MQMC model decreases more rapidly with density than ω_K from QHD for each U_{K^-} value. The curves for $\mu_n - \mu_p$ are more or less the same for both models at $\rho \lesssim 4\rho_0$; but at $\rho > 4\rho_0$, $\mu_n - \mu_p$ decreases faster in QHD. Thus the intersection and kaon condensation occur at lower densities in the MQMC model. This behavior of the intersection in Fig. 2 is well reflected in the kaon condensation onset density $\rho_{\rm crit}$ in Fig. 1. Figure 3 shows that the σ-meson field calculated by the MQMC model is larger than that calculated by QHD. A larger σ field in the MQMC model makes m_K^* and, consequently, ω_K smaller. On the other hand, as seen in Fig. 2, $\mu_n - \mu_p$ from QHD decreases faster with density at higher densities than that from MQMC. Thus the intersection of the ω_K curve with the curve for $\mu_n - \mu_p$ occurs at lower densities with the MQMC model. Therefore, $\rho_{\rm crit}$ is smaller in the MQMC model.

Another model dependency of the results can be seen from the population of kaons, which is larger in the MQMC model. The effective mass of a kaon as a point particle is determined by σ and σ^* mesons through the relation $m_K^* = m_K - g_{\sigma K}\sigma - g_{\sigma^* K}\sigma^*$ and is plotted in Fig. 4. Since the σ fields are larger in the MQMC model (as shown in Fig. 3), the effective mass and energy of a kaon are smaller in the MQMC model than in the QHD. Thus, kaon condensation takes place more in the MQMC model.

Figures 3 and 4 also show that even though σ-meson field from the MQMC model is larger than that from the QHD

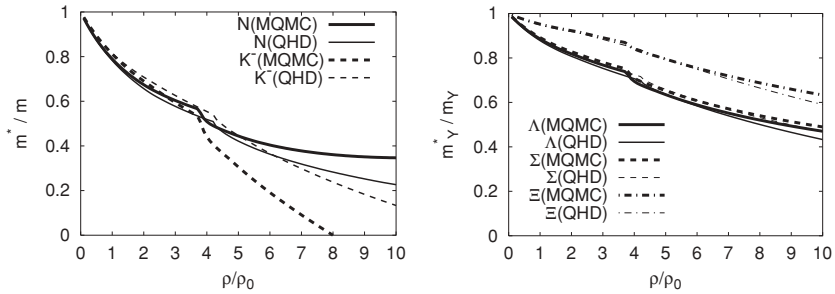

FIG. 4. Effective masses of nucleons, kaon, and hyperons plotted for $U_{K^-} = -140$ MeV.

as the densities increase, the reduction of the effective mass of baryons is smaller (or similar) with the MQMC model. If one could parametrize the effective mass of baryons from the MQMC model in the form of $m_B^* = m_B - g_{\sigma B}(\sigma)\sigma - g_{\sigma^* B}(\sigma^*)\sigma^*$, where $g_{\sigma B}(\sigma)$ and $g_{\sigma^* B}(\sigma^*)$ are functions of σ and σ^*, respectively, the results in Fig. 4 might imply that $g_{\sigma B}(\sigma)$ and $g_{\sigma^* B}(\sigma^*)$ are decreasing functions with respect to the density. The rate of decrease is rather high, since the product $[g_{\sigma B}(\sigma)\sigma]_{\rm MQMC}$ is smaller than (or similar to) $[g_{\sigma B}\sigma]_{\rm QHD}$, while the σ-field value from MQMC is much greater than that from QHD. Such a decrease of $g_{\sigma B}(\sigma)$ in the MQMC model may be regarded as partial restoration of the chiral symmetry at high densities.

We have calibrated both the MQMC and QHD model parameters to the same saturation properties. However, we find that the neutron star matter composition profiles from the two models are quite different, and that they show significant model dependence. QHD assumes the baryons as point particles, whereas the MQMC model treats the baryons as MIT bags. Thus, the major difference between the two models is in the definition of the effective mass of baryons, m_B^*. The equation of motion for the σ-meson field is also different accordingly. m_B^* in QHD is a simple linear function of the σ field, and the factor $C_B(\sigma)$ in Eq. (18) is a constant. In the MQMC model, m_B^* is a nonlinear function of the σ field, and thus $C_B(\sigma)$ is highly nonlinear. When these nonlinear quantities m_B^* and $C_B(\sigma)$ are expanded in powers of the σ field, an infinite number of σ-field terms would appear. (Cubic and quartic terms are explicitly taken into account in the QHD model as in Eq. (9).) Higher order terms can be interpreted as higher order contributions such as self-interactions of meson fields, which are believed to be more important at high densities. But at high densities, it can be questioned whether the nonlinear terms of the σ meson in the MQMC model account for the higher order effects properly and consistently. For instance, it is generally known that as the baryons come closer to each other, the interplay of heavy mesons becomes more important. At high enough densities, their self-interaction contributions may need to be included on the same ground as for the σ meson, but the present MQMC model truncates the heavy meson terms at the leading order.

It seems worthwhile to discuss at this point two more aspects of our results. The first one is the equation of state (EoS) and the resulting mass-radius relation of the neutron star. The second point is the dependence of our results on the Σ hyperon interaction in matter, which is not yet well known.

Let us first consider the EoS and the maximum mass of the neutron star. As the kaon (K^-) appears and condensates, the number of negatively charged hyperons decreases to satisfy the charge neutrality. The decrease in the number of baryons will result in the reduction of the pressure and lead to a softening of the EoS. Figure 5 shows such a softening of the EoS due to the kaon condensation. In calculating the EoS of a system consisting of multicomponent substances, as in the case with the kaon condensation, the Gibbs condition has to be employed for the proper description of the mixed phase. The curves in Fig. 5 are the results obtained with the QHD and Gibbs condition. As kaons appear, the EoS becomes considerably soft, and the effect becomes more pronounced with a stronger attraction, i.e., for a larger $|U_{K^-}|$ value. For the MQMC model, however, applying the Gibbs conditions does not give us a converging solution. Solving the 16 highly nonlinear equations together with Gibbs conditions doubled the number of equations to be solved, and the convergence could not be reached. It is not clear to us whether the convergence problem is due to numerical problems or to nonlinearity which can cause bifurcation or chaos. Therefore, we used a Maxwell construction for the MQMC model. (Some literature [46] shows that Maxwell construction is a good approximation to the Gibbs condition; but in some other literature [41], it was emphasized that the Gibbs condition produces significantly different results from those of Maxwell construction. Below we show that in our case the neutron star mass itself does not change much whether we use Maxwell or Gibbs conditions for QHD. Thus our use of Maxwell construction for the MQMC model may be considered as an acceptable approximation.) We solve the Tolman-Oppenheimer-Volkoff equation to calculate the maximum mass of a neutron star. The results are shown in Table V, where the central density, maximum mass, and corresponding radius are listed for both MQMC and QHD models. The maximum mass calculated with QHD model is

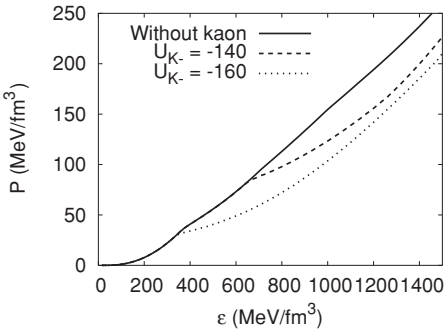

FIG. 5. Comparison of the EoS with and without kaons in QHD model. The Gibbs condition is used to treat the mixed phase.

TABLE V. Maximum mass of a neutron star M, corresponding radius R (in km), and density at the center of the star ρ_c for various U_{K^-}, for Maxwell (Mx) and Gibbs (Gb) conditions.

U_{K^-} (MeV)	MQMC (Mx)			QHD (Mx)			QHD (Gb)		
	ρ_c/ρ_0	$M/M_\odot$	R	ρ_c/ρ_0	$M/M_\odot$	R	ρ_c/ρ_0	$M/M_\odot$	R
−120	6.2	1.61	11.8	6.1	1.50	11.4	6.1	1.50	11.4
−140	4.6	1.53	12.8	5.0	1.46	12.1	5.0	1.45	12.1
−160	4.6	1.45	13.1	4.0	1.32	12.7	4.3	1.19	12.3

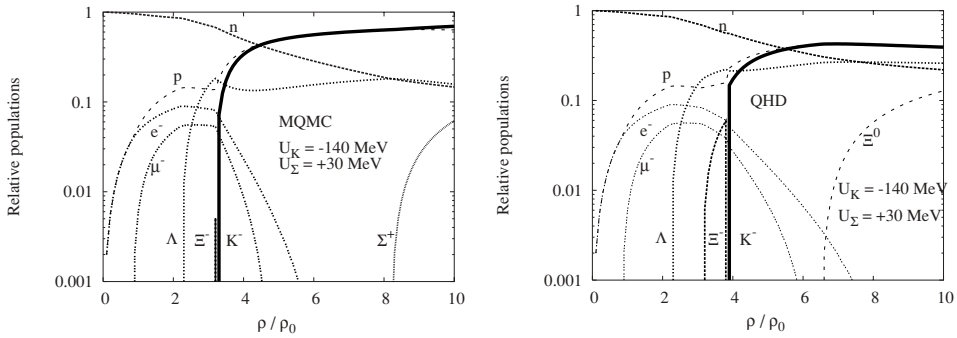

FIG. 6. Comparison of the population from the MQMC (left) with that of the QHD (right). Calculations were done with $U_\Sigma = +30$ MeV and $U_{K^-} = -140$ MeV.

roughly 10% smaller than that with MQMC model. For both models, the maximum mass becomes smaller for a larger $|U_K|$. The maximum mass calculated with MQMC and $|U_{K^-}| = 160$ MeV is compatible with observation, while the maximum mass calculated with QHD and $|U_{K^-}| = 160$ MeV becomes too small to be compatible with the observed values. However, this fact may not necessarily rule out the possibility of $|U_{K^-}|$ becoming as large as 160 MeV because there are other possible mechanisms which are not included.

Now let us consider the second aspect mentioned above. In the calculations made so far, we have assumed the quark-counting rule in determining the hyperon-meson coupling constants. Experiments on Λ hypernuclei indicate that quark counting is a good approximation of the realistic interaction of Λ hyperons in nuclei, which gives the value of Λ optical potential at saturation density in the range $-40 \sim -30$ MeV. On the other hand, there is large ambiguity in the Σ hyperon interaction strength. Reference [47] shows that Σ hyperon feels repulsion rather than attraction in a nuclear medium. There are also experimental indications that the Σ hyperon interaction is repulsive [48]. If the Σ interaction is indeed repulsive, the population profile of neutron star matter can change significantly from what was shown earlier in this work, since we have used the quark counting rule. The number of Σ^- is closely related to the onset of K^- condensation, since they compete with each other for the charge neutrality condition. To see the effect of the possible repulsive nature of the Σ interaction on the kaon condensation, we repeated the calculations with a repulsive Σ interaction. We first fit the coupling constants g'^{Σ}_{σ} in MQMC and $g_{\sigma\Sigma}$ in QHD so that the Σ optical potential value at the saturation density equaled $+30$ MeV, and fixed the remaining meson-Σ coupling constants with the quark counting rule. The resulting population profiles with the kaon optical potential $U_{K^-} = -140$ MeV are shown in Fig. 6. Compared with the quark-counting results in Fig. 1, the onset of kaon condensation occurs at slightly lower densities. This minor change happens regardless of U_{K^-} value. However, the main features of kaon condensation, i.e., its onset density, fast increase of population, and dominance at high densities are not much affected by the change of Σ interaction in nuclear medium.

IV. CONCLUSIONS AND DISCUSSIONS

Using the modified quark-meson coupling model, we have obtained the composition profiles of neutron star matter, focusing on the effects of the strange particles of hyperons and kaons. Motivated by recent theoretical predictions of deeply bound kaonic states [26] and the subsequent claims of the observations of interesting peaks found in KEK [27,28], FINUDA [30], and BNL [31] experiments, we considered the large kaon optical potential U_{K^-}. By varying the value of U_{K^-}, we have investigated how the onset density of the kaon condensation and the composition of the stellar matter change. Employing the QHD model parameters which satisfy exactly the same saturation conditions as the MQMC model, we have investigated the model dependence of the results.

We observed two common features from the two model calculations. First, a larger $|U_{K^-}|$ produces a smaller onset density of the kaon condensation. This behavior is easily understood from the relation between U_{K^-} and $g_{\sigma K}$ together with the role of $g_{\sigma K}$ to the energy of the kaon ω_K. Secondly, the number of kaons rapidly increases, and the number of negatively charged hyperons is strongly suppressed. This is because the ω meson gives rise to attraction to K^-, whereas it couples to baryons repulsively.

Model dependence was also observed. The kaon condensation takes place at lower densities in the MQMC model. The number of kaons is always larger with the MQMC model for given U_{K^-} values. Larger σ-meson fields in the MQMC model can explain these behaviors. The differences in the results from the two models become more prominent at larger densities. Growing discrepancies at higher densities have their origins partly in the effective mass of baryons in each model, which greatly affects the self-consistency condition of the σ meson. The factor $C_B(\sigma)$ in the self-consistency condition of the σ meson is highly nonlinear in the MQMC model, which can be interpreted as an infinite number of σ-meson self-interaction terms. These higher order terms may require more proper and consistent treatment at high densities.

An important issue in the dense matter physics is the restoration of the chiral symmetry. According to Ref. [49], not only the mass but also the pion decay constant and meson-nucleon coupling constants decrease at a similar ratio at around the nuclear saturation density. In Ref. [50], the idea of scaling behavior is applied to the neutron star matter using MQMC and QHD models with only nucleon degrees of freedom, and it is shown that the equation of state becomes stiffer when scaling effects are considered. This implies that if we include a scaling behavior in our present models, it may ignite the onset of exotic states earlier than the present results which do not include a scaling.

In the kaon sector, the coupling constants of a kaon and exchange mesons are currently an important issue. We took various values of the optical potential of K^- as input to fix $g_{\sigma K}$. Other kaon-meson coupling constants are fixed from naive quark counting. It is known, however, that the K^+ potential is repulsive with the magnitude $U_{K^+} \sim 10$ MeV at the saturation density [51]. If U_{K^+}, as well as U_{K^-}, is used as an input, then $g_{\sigma K}$ and $g_{\omega K}$ can be determined uniquely. For instance, if we take $U_{K^-} = -120$ and $U_{K^+} = 20$ MeV, then we get $g_{\sigma K} = 2.041$ and $g_{\omega K} = 4.187$. This value of $g_{\sigma K}(=2.041)$ is smaller than the value listed in Table IV, while $g_{\omega K}(=4.187)$ is nearly twice the $g_{\omega K}$ fixed from the quark counting. Both σ and ω mesons contribute attractively to the K^- energy, but since the ω meson becomes a dominant component at higher densities, taking into account U_{K^+} can produce appreciably different results. It may be interesting to see the effects of U_{K^+} on the kaon condensation.

In our calculations, we assumed the kaon to be a point particle in both quark and hadron models. Comparison of the two models, however, shows that whether we treat a hadron as a bag (MQMC) or a point particle (QHD) can produce a significant difference. Therefore, it is worthwhile to treat the kaon as a bag and compare the corresponding result with that of a pointlike kaon. In Ref. [45], a kaon is treated as a bag in the framework of the QMC model, but no work has been done yet with the MQMC model.

We assume m_K^* to be a linear function of σ field, but some authors employ a nonlinear form [17,44]:

$$m_K^{*2} = m_K^2 - g_{\sigma K} m_K \sigma. \tag{27}$$

If we expand this expression in powers of σ/m_K, we obtain

$$m_K^* \simeq m_K \left[1 - \frac{1}{2} g_{\sigma K} \frac{\sigma}{m_K} + O\left(\sigma^2/m_K^2\right)\right]. \tag{28}$$

The leading order term of the σ field has a factor 1/2, which is not present in Eq. (12). Due to the factor 1/2, the rate of decrease in m_K^* with density would be reduced by a factor of 2, and this would shift the kaon condensation onset density to higher densities. This dependence on the kaon Lagrangian may be worthwhile to study.

ACKNOWLEDGMENTS

S.W.H. thanks B. K. Jennings and TRIUMF for hospitality during his sabbatical leave. This work was supported by a Korea Research Foundation Grant funded by the Korean Government (MOEHRD, Basic Research Promotion Fund) (KRF-2005-206-C00007).

[1] V. R. Pandharipande, Nucl. Phys. **A178**, 123 (1971).
[2] H. A. Bethe and M. B. Johnson, Nucl. Phys. **A230**, 1 (1974).
[3] V. R. Pandharipande and R. A. Smith, Nucl. Phys. **A237**, 507 (1975).
[4] B. Friedman and V. R. Pandharipande, Nucl. Phys. **A361**, 502 (1981).
[5] J. D. Walecka, Ann. Phys. (NY) **83**, 491 (1974).
[6] V. R. Pandharipande and R. A. Smith, Phys. Lett. **B59**, 15 (1975).
[7] S. E. Thorsett and D. Chakrabarty, Astrophys. J. **512**, 288 (1999).
[8] A. R. Villarreal and T. E. Strohmayer, Astrophys. J. **614**, L121 (2004).
[9] D. J. Nice, E. M. Splaver, I. H. Stairs, O. Löhmer, A. Jessner, M. Kramer, and J. M. Cordes, Astrophys. J. **634**, 1242 (2005).
[10] S. I. A. Garpman, N. K. Glendenning, and Y. J. Karant, Nucl. Phys. **A322**, 382 (1979).
[11] A. B. Migdal, Rev. Mod. Phys. **50**, 107 (1978).
[12] D. B. Kaplan and A. E. Nelson, Phys. Lett. **B175**, 57 (1986).
[13] A. R. Bodmer, Phys. Rev. D **4**, 1601 (1971).
[14] N. Itoh, Prog. Theor. Phys. **44**, 291 (1970).
[15] G. Baym and S. A. Chin, Phys. Lett. **B62**, 241 (1976).
[16] B. D. Keister and K. S. Kisslinger, Phys. Lett. **B64**, 117 (1976).
[17] R. Knorren, M. Prakash, and P. J. Ellis, Phys. Rev. C **52**, 3470 (1995).
[18] S. Pal, M. Hanauske, I. Zakout, H. Stöcker, and W. Greiner, Phys. Rev. C **60**, 015802 (1999).
[19] N. K. Glendenning, Phys. Rev. D **46**, 1274 (1992).
[20] A. Cieply, E. Friedman, A. Gal, and J. Mares, Nucl. Phys. **A696**, 173 (2001).
[21] N. Kaiser, P. B. Siegel, and W. Weise, Nucl. Phys. **A594**, 325 (1995).
[22] J. Schaffner-Bielich, V. Koch, and M. Effenberger, Nucl. Phys. **A669**, 153 (2000).
[23] A. Ramos and E. Oset, Nucl. Phys. **A671**, 481 (2000).
[24] E. Friedman, A. Gal, and C. J. Batty, Nucl. Phys. **A579**, 578 (1994).
[25] C. J. Batty, E. Friedman, and A. Gal, Phys. Rep. **287**, 385 (1997).
[26] T. Yamazaki and Y. Akaishi, Phys. Lett. **B535**, 70 (2002); Y. Akaishi and T. Yamazaki, Phys. Rev. C **65**, 044005 (2002) .
[27] T. Suzuki, H. Bhang, G. Franklin, K. Gomikawa, R. S. Hayano, T. Hayashi, K. Ishikawa, S. Ishimoto, K. Itahashi, M. Iwasaki, T. Katayama, Y. Kondo, Y. Matsuda, T. Nakamura, S. Okada, H. Outa, B. Quinn, M. Sato, M. Shindo, H. So, P. Strasser, T. Sugimoto, K. Suzuki, S. Suzuki, D. Tomono, A. M. Vinodkumar, E. Widmann, T. Yamazaki, and T. Yoneyama, Phys. Lett. **B597**, 263 (2004).
[28] T. Suzuki, H. Bhang, G. Franklin, K. Gomikawa, R. S. Hayano, T. Hayashi, K. Ishikawa, S. Ishimoto, K. Itahashi, M. Iwasaki, T. Katayama, Y. Kondo, Y. Matsuda, T. Nakamura, S. Okada, H. Outa, B. Quinn, M. Sato, M. Shindo, H. So, P. Strasser, T. Sugimoto, K. Suzuki, S. Suzuki, D. Tomono, A. M. Vinodkumar, E. Widmann, T. Yamazaki, and T. Yoneyama, Nucl. Phys. **A754**, 375c (2005).
[29] M. Iwasaki, Talk at IX International Conference on Hypernuclear and Strange Particle Physics, 10–14, Oct. 2006, Mainz, Germany.
[30] M. Agnello, G. Beer, L. Benussi, M. Bertani, S. Bianco, E. Botta, T. Bressani, L. Busso, D. Calvo, P. Camerini, P. Cerello, B. Dalena, F. De Mori, G. D'Erasmo, D. Di Santo, F. L. Fabbri, D. Faso, A. Feliciello, A. Filippi, V. Filippini, E. M. Fiore, H. Fujioka, P. Gianotti, N. Grion, V. Lucherini, S. Marcello, T. Maruta, N. Mirfakhrai, O. Morra, T. Nagae, A. Olin, H. Outa, E. Pace, M. Palomba, A. Pantaleo, A. Panzarasa, V. Paticchio, S. Piano, F. Pompili, R. Rui, G. Simonetti, H. So, S. Tomassini, A. Toyoda, R. Wheadon, and A. Zenoni, Phys. Rev. Lett. **94**, 212303 (2005).

[31] T. Kishimoto, T. Hayakawa, S. Ajimura, S. Minami, A. Sakaguchi, Y. Shimizu, R. E. Chrien, M. May, P. Pile, A. Rusek, R. Sutter, H. Noumi, H. Tamura, M. Ukai, Y. Miura, and K. Tanida, Nucl. Phys. **A754**, 383c (2005).
[32] J. Mares, E. Friedman, and A. Gal, Nucl. Phys. **A770**, 84 (2006).
[33] X. Jin and B. K. Jennings, Phys. Lett. **B374**, 13 (1996); Phys. Rev. C **54**, 1427 (1996) .
[34] S. Banik and D. Bandyopadhyay, Phys. Rev. C **64**, 055805 (2001).
[35] B. D. Serot and J. D. Walecka, Adv. Nucl. Phys. **16**, 1 (1986).
[36] S. Fleck, W. Bentz, K. Shimizu, and K. Yazaki, Nucl. Phys. **A510**, 731 (1990).
[37] K. Saito and A. W. Thomas, Phys. Lett. **B327**, 9 (1994).
[38] K. Saito, K. Tsushima, and A. W. Thomas, Prog. Part. Nucl. Phys. **58**, 1 (2007).
[39] C. Y. Ryu, C. H. Hyun, J. Y. Lee, and S. W. Hong, Phys. Rev. C **72**, 045206 (2005).
[40] J. Boguta and A. R. Bodmer, Nucl. Phys. **A292**, 413 (1977).
[41] N. K. Glendenning and J. Schaffner-Bielich, Phys. Rev. C **60**, 025803 (1999).
[42] I. Zakout, W. Greiner, and H. R. Jaqaman, Nucl. Phys. **A759**, 201 (2005).
[43] T. A. Armstrong *et al.* (WA76 Collaboration), Z. Phys. C **51**, 351 (1991).
[44] J. Schaffner and I. N. Mishustin, Phys. Rev. C **53**, 1416 (1996).
[45] D. P. Menezes, P. K. Panda, and C. Providencia, Phys. Rev. C **72**, 035802 (2005).
[46] T. Maruyama, T. Tatsumi, D. N. Voskresensky, T. Tanigawa, T. Endo, and S. Chiba, Phys. Rev. C **73**, 035802 (2006); T. Endo, T. Maruyama, S. Chiba, and T. Tatsumi, Prog. Theor. Phys. **115**, 337 (2006).
[47] J. Mares, E. Friedman, A. Gal, and B. K. Jennings, Nucl. Phys. **A594**, 311 (1995).
[48] P. K. Saha, H. Noumi, D. Abe, S. Ajimura, K. Aoki, H. C. Bhang, K. Dobashi, T. Endo, Y. Fujii, T. Fukuda, H. C. Guo, O. Hashimoto, H. Hotchi, K. Imai, E. H. Kim, J. H. Kim, T. Kishimoto, A. Krutenkova, K. Maeda, T. Nagae, M. Nakamura, H. Outa, T. Saito, A. Sakaguchi, Y. Sato, R. Sawafta, M. Sekimoto, Y. Shimizu, T. Takahashi, H. Tamura, L. Tang, K. Tanida, T. Watanabe, H. H. Xia, S. H. Zhou, X. F. Zhu, and L. H. Zhu, Phys. Rev. C **70**, 044613 (2004).
[49] G. E. Brown and M. Rho, Phys. Rev. Lett. **66**, 2720 (1991).
[50] C. H. Hyun, M. H. Kim, and S. W. Hong, Nucl. Phys. **A718**, 709c (2003); C. Y. Ryu, C. H. Hyun, S. W. Hong, and B. K. Jennings, Eur. Phys. J. A **24**, 149 (2005) .
[51] G. Q. Li, C.-H. Lee, and G. E. Brown, Phys. Rev. Lett. **79**, 5214 (1997).